

Origin and Evolution of the Abundance Gradient along the Milky Way Disk

J. Fu^{1,2}, J.L. Hou¹, J. Yin^{1,2} and R.X. Chang¹

¹*Key Laboratory for Research in Galaxies and Cosmology, Shanghai Astronomical Observatory, the Chinese Academy of Sciences, 80 Nandan Road, Shanghai, 200030, China*

²*Graduate School, the Chinese Academy of Sciences, Beijing, 100039, China*

fujian@shao.ac.cn; houjl@shao.ac.cn; jyin@shao.ac.cn, crx@shao.ac.cn

ABSTRACT

Based on a simple model of the chemical evolution of the Milky Way disk, we investigate the disk oxygen abundance gradient and its time evolution. Two star formation rates (SFRs) are considered, one is the classical Kennicutt-Schmidt law ($\Psi = 0.25\Sigma_{\text{gas}}^{1.4}$, hereafter C-KS law), another is the modified Kennicutt law ($\Psi = \alpha\Sigma_{\text{gas}}^{1.4}(V/r)$, hereafter M-KS law). In both cases, the model can produce some amount of abundance gradient, and the gradient is steeper in the early epoch of disk evolution. However, we find that when C-KS law is adopted, the classical chemical evolution model, which assumes a radial dependent infall time scale, cannot produce a sufficiently steep present-day abundance gradient. This problem disappears if we introduce a disk formation time scale, which means that at early times, infalling gas cools down onto the inner disk only, while the outer disk forms later. This kind of model, however, will predict a very steep gradient in the past. When the M-KS law is adopted, the model can properly predict both the current abundance gradient and its time evolution, matching recent observations from planetary nebulae and open clusters along the Milky Way disk. Our best model also predicts that outer disk (artificially defined as the disk with $R_g \geq 8kpc$) has a steeper gradient than the inner disk. The observed outer disk gradients from Cepheids, open clusters and young stars show quite controversial results. There are also some hints from Cepheids that the outer disk abundance gradient may have a bimodal distribution. More data is needed in order to clarify the outer disk gradient problem. Our model calculations show that for an individual Milky Way-type galaxy, a better description of the local star formation is the modified KS law.

Subject headings: Stars:abundances - Galaxy:gradient - Galaxy:evolution

1. Introduction

The radial abundance gradient of a disk galaxy is an essential ingredient in an accurate picture of galaxy formation and evolution. During the past twenty years, the existence of an abundance gradient along the Milky Way disk has been well established by observations using various tracers. An oxygen and/or iron abundance gradient of about $-0.05 \sim -0.07$ dex kpc^{-1} was obtained by observing young stars and HII regions (see Hou & Chang 2001; Rudolph et al. 2006 and references therein), planetary nebulae (Maciel et al. 2005; 2006) and open clusters (Friel 1995, 1999; Carraro et al. 1998; Chen et al. 2003). Two spiral neighbors of the Milky Way Galaxy in the Local Group, M33 and M31 have provided further evidence for the existence of disk abundance gradient. A relatively flatter gradient is observed for M31, which is about $-0.04 \sim -0.05$ dex kpc^{-1} (Dennefeld et al. 1981; Blair et al. 1982). As for M33, the observed value of oxygen abundance gradient diverges greatly at present. Different observers have presented different values based on various objects (mainly HII regions and B stars). Published data show that the oxygen gradient varies from -0.02 dex kpc^{-1} to -0.16 dex kpc^{-1} (Magrini et al. 2007a). A larger and more homogeneous sample of HII regions that covers the whole M33 disk is needed in order to get conclusive results about the real gradients. Such a project is currently undergoing by a couple of groups (Rosolowsky & Simon 2008; Magrini et al. 2007b).

Nevertheless, it is important to point out that the abundance gradients for different elements are sometimes different due to different nucleosynthetic history, and the exact values for the Milky Way disk are still not very certain (Deharveng et al. 2000; Daflon & Cunha 2004; Carraro et al. 2007). This has prevented the chemical evolution models from being constrained clearly.

Another question is how the abundance gradient along a Galaxy disk evolves during the history of disk evolution. With the help of large samples of Open Clusters (OCs) and Planetary Nebulae (PNe), it is now possible to explore this question observationally. The estimated ages of OCs and PNe of various types span a large fraction of the age of the Galaxy. Observations of the abundances of those objects across the Milky Way disk have provided some important information on the past history of the abundance gradients. Indeed, current data show that the gradient was steeper in the past (Carraro et al. 1998, 2007; Hou et al. 2002; Chen et al. 2003; Maciel et al. 2003, 2005, 2006; Magrini et al. 2008).

The observed disk abundance gradient and its evolution offer the opportunity to test theories of disk chemical evolution and stellar nucleosynthesis. Detailed knowledge about the disk abundance gradient and its time evolution are crucial not only in our understanding of the metal enrichment history along the disk, that is the star formation history, but also very important in our understanding of the metallicity relationship between high redshift

Damped Lyman Alpha systems and local disks (Wolfe et al. 2005; Hou et al. 2005). In the framework of a phenomenological scenario of disk formation, several mechanisms may play roles in shaping the abundance gradient and its evolution. One is the star formation processes in the disk. Observations of local disk and starburst galaxies show that the star formation rate (SFR) per unit area is proportional to some power of the gas mass surface density (Kennicutt 1998). This non-linear star formation law may result in and largely influence the building of radial abundance gradients. Another mechanism is the so-called “inside-out” disk formation. In most classical chemical evolution models, it is generally assumed that the disk forms by gas infalling from the outer halo, and that the infall can be described by an exponential law, in which the infall time scale is always assumed to be radially dependent $\tau = \tau(r)$, with a smaller value in the inner region and a much larger one in the outer disk (Chang et al. 1999; Boissier & Prantzos 1999; Hou et al. 2000; Chiappini et al. 2001). On the other hand, many observations show that radial truncation exists in most disk galaxies (e.g. Pohlen et al. 2002), which means there is a change in the slope of total mass surface density and gas mass surface density from a shallow exponential disk to a much steeper one (de Grijs et al. 2001). This truncation radius r_t appears to evolve with the redshift z of a galaxy (Azzollini et al. 2008), which is a strong indication that the disk grows from smaller to larger. For a simple phenomenological disk formation model, this property could be described by a disk formation time scale t_0 , which is proportional to the radius from the galaxy center. In both cases of $\tau(r)$ and t_0 , there is a rapid increase of the metal abundance during the early epochs in the inner disk, leading to a steep abundance gradient. As time goes on, star formation “migrates” to the outer disk, producing metals and flattening the abundance gradient there.

However, the mechanisms mentioned above could work together. It is difficult to distinguish which one plays a more important role, or if the scenario may be different for various disk galaxies. The purpose of this paper is to understand which mechanism plays the most important role in the origin and evolution of disk abundance gradients in a galactic chemical evolution model. We concentrate on the Milky Way disk because there are various observations on its disk abundance, especially the recent PNe data (Maciel et al. 2003, 2005, 2006) and open clusters (Chen et al. 2003; Carraro et al. 2007), which provide unique constraints on time evolution of the disk abundance gradient and that could be sensitive to different model assumptions. In section 2, we will describe the main content of our model, which includes the mechanisms mentioned above. In section 3, the resulting model radial profiles will be given, and the effect of τ , SFR, and t_0 on the abundance gradient and its evolution will be analyzed. The best model will be decided by comparing the model results with the observational data. Finally, the main results will be summarized in section 4.

2. The Model

We assume that the Milky Way has been embedded in a dark matter halo. Primordial gas within the dark halo cools down to form a rotationally supported disk, which is assumed to be sheet-like and a system of a series of independent rings with the width of 500 pc. The ring centered at $r_{\odot} = 8$ kpc is labeled as the solar neighborhood. Star formation and chemical evolution proceed in each ring due to infalling gas.

2.1. Infall Rate and Disk Formation Process

The assumption of a gas infall process is traditionally based upon the need to explain the locally observed metallicity distribution of long-lived stars, which cannot be explained by the simple “closed-box” model (leading to the well-known “G-dwarf problem”, Pagel 1989). Recent observations show that the Milky Way disk (and also M31, M33) is currently accreting substantial amounts of gas with low metallicity ($\sim 1 \text{ M}_{\odot}\text{yr}^{-1}$) from high velocity clouds (Blitz et al. 1999; Ferguson et al. 2002; Thilker et al. 2004; Ibata et al. 2005; van den Bergh 2006). We note that Sancisi et al.(2008) proposed that the accreting rate of the Milky Way could be about $0.1\sim 0.2 \text{ M}_{\odot}\text{yr}^{-1}$, about ten times less than that required by the observed SFR in the disk. However, there is some evidence that the extra gas may come from a Galactic fountain (Sancisi et al. 2008).

Like many other phenomenological models, we also adopt an exponentially decaying gas infall rate $f(r, t)$ as:

$$f(r, t) = \begin{cases} A(r) e^{-[t-t_0(r)]/\tau(r)} & t \geq t_0(r) \\ 0 & t < t_0(r) \end{cases} \quad (1)$$

where $t_0(r)$ is the time when gas at radius r begins to infall onto the disk. $A(r)$ is normalized $\int_0^{t_g} f(r, t) dt = \Sigma_{\text{tot}}(r, t_g)$, where $\Sigma_{\text{tot}}(r, t_g)$ is the current total (gas+star) mass surface density, and t_g is the age of the disk. We adopt $t_g = 13.5$ Gyr for the Milky Way. That means the Milky Way Galaxy formed at the beginning of the universe. We note that the thin disk is relatively young on average, but the oldest open clusters in the disk could be as old as 10 Gyr (Chen et al. 2003; Carraro et al. 2007), while dwarf stars in the disk have ages as old as that of Galaxy. As a working hypothesis, we shall always assume that the disk is as old as the Galaxy (see also in Boissier and Prantzos 1999; Hou et al. 2000). Test calculations show that adopting a smaller disk age (for example, 11 Gyr) does not effect the main results of the model. This is reasonable since the disk evolves very little in the last several Gyr.

We assume that the current total surface density (unit: $M_{\odot}\text{pc}^{-2}$) of the disk has an exponential form:

$$\Sigma_{\text{tot}}(r, t_g) = \Sigma_{\text{tot}}(r_{\odot}, t_g)e^{-(r-r_{\odot})/r_d} \quad (2)$$

From Equations (1) and (2), we can get:

$$A(r) = \frac{\Sigma_{\text{tot}}(r_{\odot}, t_g)e^{-(r-r_{\odot})/r_d}}{[1 - e^{-[t_g-t_0(r)]/\tau(r)}] \tau(r)} \quad (3)$$

where r_d is the disk radial scale length, and $\Sigma_{\text{tot}}(r_{\odot}, t_g)$ is the total mass surface density in the solar neighborhood at the present-day. We adopt $r_d = 2.7\text{kpc}$ and $\Sigma_{\text{tot}}(r_{\odot}, t_g) = 56M_{\odot}\text{pc}^{-2}$ for the Milky Way disk (Robin et al. 1996; Boissier & Prantzos 1999; Holmberg & Flynn 2004; Hammer et al. 2007). The combination of Eq.(1) and Eq.(3) will fix the history of gas infall of disk if $t_0(r)$ and $\tau(r)$ are given.

Two cases in the above model correspond to the so-called “inside-out” disk formation scenario. One is represented by the radial dependent infall time scale, e.g. $\tau(r) = a \times r + b$ with $a > 0$, which means the infall time scale of the inner disk is shorter than that of the outer disk. The second is described by radial dependent disk formation time scale $t_0(r)$, which is somewhat similar to the time dependent disk truncation. This case, although over-simplified, is supported by both observations (Azzollini et al. 2008) and numerical simulations (Roškar et al. 2008). The real mechanisms for the formation and evolution of the disk truncation are quite complicated and not well understood (as discussed in Azzollini et al. 2008; Franx et al. 2008; Roškar et al. 2008). Here we just assume the disk size increases with time, i.e. t_0 increases with galactic-centric distance r/r_d . Thus we adopt a simple linear form:

$$t_0(r) = \gamma \times (r/r_d) \quad (4)$$

where γ is a free parameter. This assumption corresponds to the gradual build-up of the disk from the inner to the outer part. Our purpose is try to understand how this disk truncation influences the disk abundance gradient evolution. In Section 3, we shall discuss how $t_0(r)$ and $\tau(r)$ affect the build-up of radial abundance gradient.

2.2. Star Formation Law

Kennicutt (1998) has shown that the global SFRs of disks and circumnuclear starburst galaxies are correlated with the local gas density. The entire range of investigated galaxies, spanning a magnitude of 5-6 orders in gas mass and SFR surface densities, fits on a common power law with index $n \sim 1.4$. The tight relation shows that a simple Schmidt (1959) power law provides an excellent empirical parameterization of the SFR across an enormous

range of SFRs. It also suggests that the gas density is the primary determinant of the SFR on these scales. Models of galaxy formation and evolution usually adopt this best-fitting Kennicutt-Schmidt law (hereafter, Classical KS law):

$$\Psi(r, t) = 0.25 \Sigma_{\text{gas}}^n(r, t) \quad (5)$$

where Σ_{gas} is in unit of $\text{M}_{\odot} \text{pc}^{-2}$. $\Psi(r, t)$ is in unit of $\text{M}_{\odot} \text{pc}^{-2} \text{Gyr}^{-1}$, $n = 1.4 \pm 0.15$.

From the observational point of view, Kennicutt (1998) also found a correlation between the observed SFR and the ratio of the surface gas density to the local dynamical time scale, $\Sigma_{\text{gas}}/\tau_{\text{dyn}}$. In particular, from this correlation one can derive the following parametrization:

$$\Psi(r, t) \propto \frac{\Sigma_{\text{gas}}}{\tau_{\text{dyn}}} \propto \Sigma_{\text{gas}} \Omega \quad (6)$$

where Ω is the angular rotation speed of the gas. Since $\Omega \sim V(r)/r$, the SFR could be expressed as $\Psi(r, t) \propto \Sigma_{\text{gas}} \frac{V(r)}{r}$, where $V(r)$ is the disk circular velocity at radius r .

In Boissier & Prantzos (1999), the SFR was also expressed as (hereafter, Modified KS law):

$$\Psi(r, t) = \alpha \Sigma_{\text{gas}}^n \left[\frac{V(r)}{220} \right] \left[\frac{r}{r_{\odot}} \right]^{-1} \quad (7)$$

where Σ_{gas} is in unit of $\text{M}_{\odot} \text{pc}^{-2}$, $V(r)$ is in unit of km s^{-1} , r is in unit of kpc. The index n is chosen to be ~ 1.5 on an empirical basis. And for the Milky Way disk, $\alpha = 0.1$, $V(r) = V_{\text{max}} = 220 \text{km s}^{-1}$. They also adopted this Modified KS law in subsequent models for external spirals, and their models can successfully reproduce the global properties of spirals (Boissier & Prantzos 2000, 2001; Boissier et al. 2001).

Concerning the average properties of SFR and gas mass surface densities, the Classical KS law was further supported by recent observations. Boissier et al. (2007) have investigated 43 nearby, late-type galaxies from GALEX and conclude that, on the average, their results are compatible with Classical KS law and can extend this simple law to much lower gas mass surface density. But for an individual galaxy, some will show a very untypical pattern in the $\lg(\text{SFR})-\lg(\Sigma_{\text{gas}})$ plot, e.g. the M31 disk, as pointed out by Boissier et al. (2007) and Yin et al. (2008).

In an earlier paper, Molla et al. (1997) also investigated the radial abundance distributions for a number of nearby spirals, including the Milky Way. In treating the star formation processes for different galaxies, they considered the radially dependent efficiency for the formation of molecular clouds. The efficiencies are allowed to change from galaxy to galaxy. In this work, we have simply adopted the classical KS law (Eq.(5), Kennicutt 1998) and modified KS law (Eq.(7)), where the later case is equivalent to a radial dependent efficiency of

star formation. This kind of modified SFR has been extensively adopted during the past for chemical evolution studies of the Milky Way disk (see review by Matteucci 2001). But this is not to say that the classical K-S law does not properly describe disk galaxies. In fact, the classical KS law has been widely accepted for the average star formation properties of a galaxy. In many studies, especially in semi-analytic modeling of disk galaxies, the classical K-S law is often adopted. The recent space resolved observations for M51a by Kennicutt et al. (2007) show that the index is comparable with the classical KS law, but this does not mean it is valid for all individual galaxies, especially in the past history of a galaxy. A comparison study is needed based on the disk evolution history. The time evolution of the abundance gradient and how it changes with galactocentric distance are good constraints. These kind of constraints have been used less often because there are fewer observational constraints. Our purpose is to try to understand which kind of SFR is more suitable to describe the local star formation properties in the Milky Way disk by calculating the evolution history of the disk abundance gradient.

2.3. Chemical Evolution

The galactic disk is considered as an ensemble of concentric, independently evolving rings, progressively built up by infall of primordial composition. For the purpose of simplicity, we adopt the Instantaneous Recycling Approximation (IRA). Therefore, the chemical evolution at each ring can be followed by solving these appropriate set of integro-differential equations (Prantzos 2008):

$$\begin{cases} \frac{d}{dt} \Sigma_{\text{gas}} = -(1 - R) \Psi + f \\ \frac{d}{dt} (X_i \Sigma_{\text{gas}}) = -X_i \Psi + E_i \end{cases} \quad (8)$$

Table 1. Parameters Adopted in the Models

Parameters	Values	References
r_d (kpc)	2.7	Robin et al. (1996)
R	0.32	Kroupa et al. (1993)
$12 + \log (\text{O}/\text{H})_{\odot}$	8.7	Lodders (2003)
$\Sigma_{\text{tot}}(r_{\odot}, t_g)$ ($M_{\odot} \text{pc}^{-2}$)	56	Holmberg & Flynn (2004)
t_g (Gyr)	13.5	WMAP3
y_i	$(X_i)_{\odot}$	

where X_i is the mass abundance of element i ; R is the return fraction; E_i is the rate at which dying stars restore both the enriched and unenriched material into the ISM. When IRA is adopted, $E_i = y_i\Psi + (X_i - y_i)\Psi R$, where y_i is the yield of element i and we adopt $y_i = (X_i)_\odot$ throughout this paper. Adopting z stellar Initial Mass Function (IMF) as a multi-slope power-law between $0.1 M_\odot$ and $100 M_\odot$ from the work of Kroupa et al. (1993), we can get $R = 0.32$.

The metals predicted by the model are compared with observed abundances of alpha elements (e.g. oxygen), which are mainly produced by SN II explosions of massive stars. In this paper, when we compare with the observed abundance gradients, we mainly refer to oxygen abundance. We shall convert the abundance gradient of iron from open clusters to that of oxygen according to the calibration of Maciel et al. (2005).

3. Model Parameters and Results

The input parameters adopted in the model are listed in Tab.1. In order to distinguish which mechanism plays the most important role in the origin and evolution of abundance gradients, we adopt 3 models for different SFRs and disk formation time scale prescriptions which are listed in Tab.2. In each Model, three forms of the infall time scale are considered. One is $\tau = 1.0\text{Gyr}$ ($\tau = 0$ is not adopted for it is the “closed-box” model which leads to G-dwarf problem) and another one is $\tau = \infty$, both of which represent extreme cases for constant infall time scale. The third one is “inside-out” scenario, we adopt $\tau(r) = 0.75 \times r + 1$ (Gyr), where r is in unit of kpc.

3.1. Radial Profiles of Gas, Star and SFR

The results for the present-day radial profiles of the 3 models are plotted in Fig.1. These profiles include gas mass surface density Σ_{gas} , stellar mass surface density Σ_{star} , star

Table 2. SFR and timescales for three models

Model	SFR	$t_0(r) = \gamma \frac{r}{r_d}$	$\tau(r)$ (Gyr)
Mod-A	Classical KS law	$\gamma = 0$	$1.0, \infty, 0.75r + 1$
Mod-B	Classical KS law	$\gamma = 1.9$	$1.0, \infty, 0.75r + 1$
Mod-C	Modified KS law	$\gamma = 0$	$1.0, \infty, 0.75r + 1$

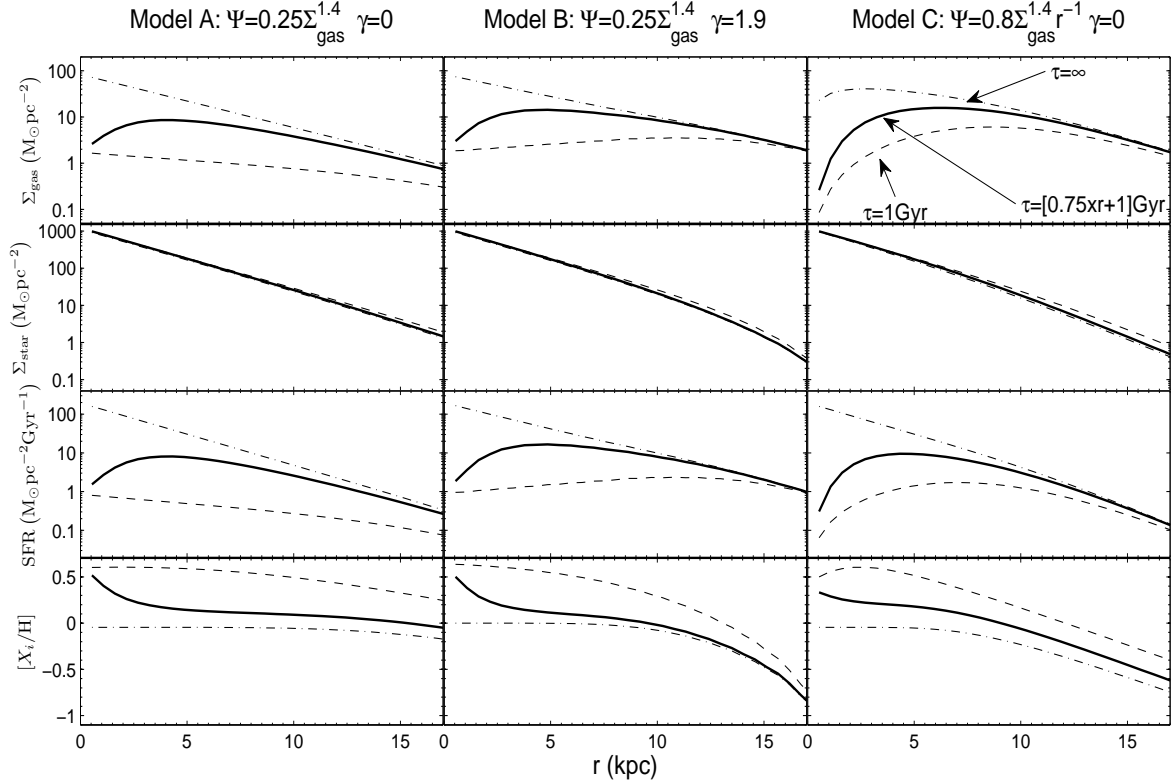


Fig. 1.— The current radial profiles of gas mass surface density Σ_{gas} ($M_{\odot}\text{pc}^{-2}$), stellar mass surface density Σ_{star} ($M_{\odot}\text{pc}^{-2}$), star formation rate ($M_{\odot}\text{pc}^{-2}\text{Gyr}^{-1}$), and abundance $[X_i/\text{H}]$ of element i . Three columns represent 3 models mentioned above, which are labeled on the top. Disk formation time scale is given by $t_0(r) = \gamma \times r/r_d$. Infall time scale is given by $\tau(r) = 0.75 \times r + 1$ (Gyr) (solid line). In all panels, the dashed and dash-dotted lines represent $\tau = 1$ Gyr and $\tau = \infty$ respectively under constant τ assumption.

formation rate and abundance $[X_i/\text{H}]$ of element i . In all panels of Fig.1, the dashed and dash-dotted curves are two limits of the constant τ : dashed ones represent $\tau = 1\text{Gyr}$ and dash-dotted ones represent $\tau = \infty$. Results of other constant τ are between the two limits. The results of the “inside-out” scenario are plotted with solid lines.

From Fig.1, we can see that a curve of radially dependent $\tau(r)$ is actually the ensemble of points on curves of different constant τ , and each point at an arbitrary radius r' is the point at r' on the curve of constant $\tau = \tau(r')$. Thus no matter what form of $\tau(r)$ is adopted, the radial profiles of all quantities from radius dependent $\tau(r)$ are between the profiles of maximum and minimum constant τ . From Fig.1, we can also find that the shape of a radial profile is mainly determined by the adopted form of SFR and $t_0(r)$, while different values and forms of $\tau(r)$ give similar profiles. We also notice that Model C predicts a deep central

depression of the gas mass surface density as long as the infall time scale is not too big. This is because the equivalent star formation efficiency (that is $\alpha \times (1/r)$) is inversely proportional to the distance from the galaxy center, therefore, there is a large and fast consumption of infalling gas in the inner disk.

3.2. Radial Abundance Gradients

We calculate the current abundance gradients $\frac{d[X_i/H]}{dr}$ from the inner part, $r = 4.0$ kpc, to the outer part, $r = 16.2$ kpc, of the disk. This range is defined as the whole disk, which is chosen in order to be consistent with most of the observations. We also divide the disk into inner and outer parts with the intersection at solar position $r_\odot = 8$ kpc. The results for all 3 models are listed in Tab.3. We shall discuss the effect of $\tau(r)$, $t_0(r)$ and SFR on the abundance gradients, respectively. Test calculations show that changing the outer disk radius (for example, up to 21 kpc, about $8r_d$) does not affect the main conclusions discussed below.

Infall Time Scale, $\tau(r)$: From Tab.3, we find that in all cases, for a constant infall time scale, the abundance gradients get flatter with the increase of τ value. When $\tau(r)$ is radially dependent, results are between the two extreme cases ($\tau=1$ Gyr and ∞). In Mod-A, the current gradient value is much smaller than other two cases (we will see below that Mod-A is not consistent with the observed value in the Milky Way disk). In Mod-B and C, the gradient values of the whole disk are similar for different infall time scale. We will see below that compared with the role of SFR and disk formation time scale $t_0(r)$, infall time scale plays minor role in shaping the abundance profile in the Milky Way disk.

Disk Formation Time Scale, $t_0(r)$: Now, we turn to the disk formation time scale t_0 . In Mod-B, we adopt the same SFR form as in Mod-A (Classical KS law), but we introduce the disk formation time scale $t_0(r)$. From Fig.1 and Tab.3, we find that the Classical KS law with an appropriate $t_0(r)$ (hereafter we assume $t_0(r) = 1.9 \times r/r_d$ Gyr) will produce an abundance gradient consistent with the observation in the Milky Way disk ($-0.05 \sim -0.07$ dex kpc^{-1}). We can also see that different infall time scales do not affect the final gradient much.

Star Formation Rate: In Mod-C, we have adopted the modified KS star formation law, that is the radially dependent SFR. But we do not introduce the disk formation time scale, i.e. $t_0(r) = 0$. From Fig.1 and Tab.3, we can see that this model can also produce a strong enough abundance gradient for a disk evolved to the present day. Again, we find that infall time scales play a minor role.

In summary, we can see that when we adopt the classical KS star formation law ($\Psi \propto \Sigma_{\text{gas}}^n$), the chemical evolution model based on the so-called “inside-out” infall time scale cannot produce an abundance gradient that is steep enough at the present day. If we introduce the disk formation time scale, then the model is able to produce a steep abundance gradient no matter how we choose the infall time scale. On the other hand, when we adopt the radial dependent star formation law, i.e. the modified KS law ($\Psi \propto \Sigma_{\text{gas}}^n r^{-1}$), the model is able to predict the required abundance gradient by choosing proper infall time scale. From the results of three models, we can find that when $t_0(r) \neq 0$, an appropriately steep abundance gradient can be produced no matter how we choose the infall time scale τ and star formation law.

In Tab.3, we also present the abundance gradients for inner and outer disk. We divide the disk into inner and outer part at radius $r_{\odot} = 8$ kpc. For all models, the outer disk has larger abundance gradient than inner part, especially in Mod-B and Mod-C. This is because in Model B, we have introduced the disk formation time scale, which results in a delayed star formation and lower metallicity in the outer disk. While in Mod-C, SFR is inversely proportional to radial distance from the galactic center, which results in lower a star formation rate and lower metal production rate in the outer disk.

On the observational side, current findings on the shape of present disk abundance gradient, especially in the outer part of the disk, are still quite controversial (see Table.4 for a compilations from the recent literature). Recent observations of the outer disk open clusters have shown a flattening of the Galactic gradient beyond 10-12kpc (Carraro et al. 2007; Yong et al. 2005). However, other studies also based on the open clusters show that the gradient of outer disk is steeper (Janes et al. 1988; Friel et al. 2002; Chen et al. 2003). Other studies based on different tracers, such as HII regions (Vilchez & Esteban 1996), Cepheids (Andrievsky et al. 2004; Lemasle et al. 2008), planetary nebulae (Costa et al. 2004), also indicate some hints of flattening gradient in the outer disk. On the other hand, there are also studies based on young stars and HII regions showing a continuous decreasing of gradient toward the outer disk (Deharveng et al. 2000; Rolleston et al. 2000).

When compared with our model predictions, an observed small gradient in the outer disk is compatible with the value from Mod-A, while a steeper gradient is consistent with Mod-C. Clearly, much work needs to be done on both observations and modeling. The time variation of the Galactic abundance gradient could provide a more comprehensive test for the different chemical evolution models than just a single measured abundance gradient at the current time. Also abundance measurements of α elements for outer disk tracers are very much needed in order to have detailed abundance ratio analysis, such as the radial variation of [O/Fe]. This is very important to understand the history of star formation in the outer disk

Table 3. Model results of current disk abundance gradient (unit: dex kpc⁻¹)

τ (Gyr)	Mod-A	Mod-B	Mod-C
whole disk: 4.0-16.2 kpc			
$\tau = 1$	-0.027	-0.091	-0.075
$\tau = \infty$	-0.009	-0.056	-0.054
$0.75 \times r + 1$	-0.015	-0.066	-0.063
inner disk: 4.0-8.0 kpc			
$\tau = 1$	-0.015	-0.040	-0.065
$\tau = \infty$	-0.001	-0.007	-0.023
$0.75 \times r + 1$	-0.013	-0.021	-0.036
outer disk: 8.0-16.2 kpc			
$\tau = 1$	-0.032	-0.115	-0.079
$\tau = \infty$	-0.013	-0.079	-0.068
$0.75 \times r + 1$	-0.017	-0.087	-0.076

Table 4. Observed abundance gradients in the outer disk

Tracers	Element	R_g (kpc)	Gradients (dex/kpc)	Refs.
Cepheids	Fe	8-12	-0.061	(1)
Cepheids	O	8-12	-0.041	(1)
Cepheids	Fe	8-12	-0.056	(1),(2)
Cepheids	O	8-12	-0.051	(1),(2)
Cepheids	Fe	10-16.4	-0.077	(2)
Cepheids	Fe	10-15	-0.012	(3)
Cepheids	Fe	10-15	-0.050	(2),(3)
Cepheids	Fe	12-17.2	-0.052	(4)
Open Clusters	Fe	8-14	-0.06	(5)
Open Clusters	Fe	12-22	-0.018	(6)
Open Clusters	α elements	12-22	-0.003~-0.019	(6)
Open Clusters	Fe	10-16	-0.047	(7)

Ref: (1)Lemasle et al. 2007; (2)Andrievsky et al. 2002; (3)Lemasle et al. 2008; (4)Yong et al. 2006; (5)Friel et al. 2002; (6)Carraro et al.2007; (7)Chen et al. 2003

since α elements are mainly produced in massive stars when they exploded as SNII, while iron is mainly synthesized from low and intermediate stars exploded as SNIa. Those two kinds of elements may have different gradient behavior. Cepheids are high-mass stars whose abundance values could be regarded as the current composition of the interstellar medium. Although a number of abundance measurements have been done by observing Cepheids in the outer disk, the current situation is still not very clear. For example, the outer disk Cepheids appear to exhibit a bimodal distribution for the $[\text{Fe}/\text{H}]$ and $[\text{O}/\text{Fe}]$ (Yong et al. 2006; Lemasle et al. 2008). The single linear radial abundance gradient is also questioned by observations from Cepheids (Andrievsky et al. 2004; Lemasle et al. 2008) and open clusters (Twarog et al. 1997). There are also alternative points of view regarding the formation history of the outer Galactic disk, in which merger events or accretions of small satellites may be responsible for the unusual metallicity distributions observed in outer open clusters and Cepheids (Yong et al. 2005). If this is the case, much sophisticated infall models are needed.

3.3. The Evolution of Abundance Gradient

As we have already mentioned above, Mod-B and C can both produce the proper current abundance gradient, which is consistent with the observed values along the Galactic disk. It is difficult to conclude which one is better.

Now we discuss the time evolution of the abundance gradient. For Mod-A and C, we calculate the gradients $\frac{d[X_i/\text{H}]}{dr}$ still from the inner part to the outer part of the disk (4.0 - 16.2 kpc) like what we do with current gradient. But for Mod-B, we calculate from the inner part (4.0 kpc) to the outermost boundary where the disk just begins to form by infall gas at time $t = t_0$. When the disk grows up to 16.2 kpc, we fix the radius range to be between 4.0 and 16.2 kpc. This is also why the curves of Model B in Fig.2 show an abrupt increase in the gradient around 11.8 Gyr, since the disk has not grown to 16.2 kpc before this stage.

The predicted evolutions of the abundance gradients for three models are plotted in Fig.2. For each model, we calculated three cases for infall time scale, as was indicated in the figure. The shaded area is the observed oxygen abundance gradient from different PN populations (Maciel et al. 2003; 2006). In Chen et al. (2003), a shallow current iron abundance gradient is derived. In checking their data, however, we find that the gradient value heavily relies on one outer young cluster at about 15 kpc. There are not enough young clusters in the sample at large radius. In order to overcome this shortage, we have combined the data of open clusters from Friel et al. (2002), Chen et al. (2003) (mainly the OCs of $r < 13\text{kpc}$) and Carraro et al. (2007) (mainly the OCs of $r > 12\text{kpc}$), then we show the

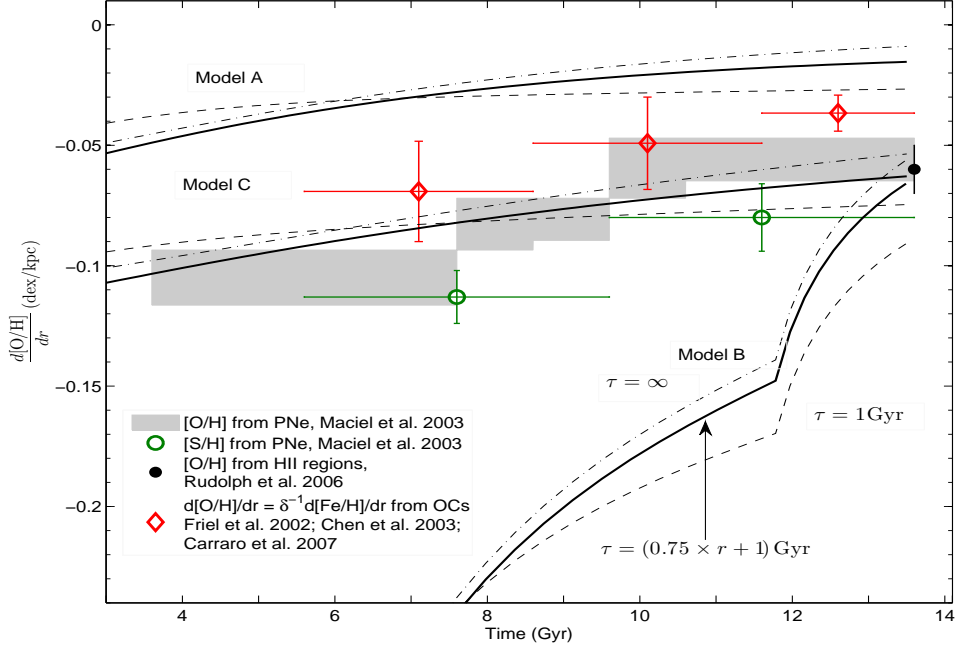


Fig. 2.— Time evolution of the radial abundance gradient. Predictions of three models (Model A, B and C) are plotted. Dashed, dash-dotted and solid lines represent different infall time scale of $\tau = 1\text{Gyr}$, $\tau = \infty$ and $\tau(r) = (0.75 \times r + 1)$ Gyr respectively. Three models show quite different history of abundance gradient. The disrupted rise in Model B at about 11.8 Gyr is caused by the disk formation time scale. The shaded area is the observed oxygen abundance gradients from PNe (Maciel et al. 2003). Open circles are sulphur abundance gradients from different aged PNe (Maciel et al. 2003). The open diamonds are oxygen abundance gradients from open clusters samples between $r = 4.0$ kpc to $r = 16.2$ kpc, which are transferred from iron abundance gradients according to the calibration of Maciel et al. (2005). In order to overcome the shortage of outer disk cluster samples in Chen et al. (2003), we have combined the data from Friel et al. (2002), Chen et al. (2003) and Carraro et al. (2007). The black point is the current oxygen abundance gradient obtained from HII regions (Rudolph et al. 2006).

evolution of gradients obtained from the samples of 4.0-16.2 kpc, where the iron gradient has been transferred to oxygen by the following calibration (Maciel et al. 2005):

$$\frac{d[12 + \log(\text{O}/\text{H})]}{dr} = \frac{1}{\delta} \frac{d[\text{Fe}/\text{H}]}{dr} \quad (9)$$

where δ is the coefficient independent of the galactocentric distance, and is about 1.0~ 1.5.

Here we adopt $\delta=1.2$ (Maciel et al. 2005).

Based on Fig. 2, we can find that:

1) All three models show that the disk abundance gradient is steeper in the early stage of disk evolution. Both Model B and C can predict acceptable current abundance gradients when they are compared with the young tracers in the Galactic disk.

2) Model A always predicts a flatter abundance gradient compared with other models at any time. It also predicts a much shallower current gradient compared with the results from young objects (e.g. HII regions from Rudolf et al. 2006; Cepheids from Yong et al. 2006). We note that there are also a number of observations showing a shallow radial abundance gradient (Deharveng et al. 2000; Daflon & Cunha 2004; Carraro et al. 2007), but the absolute values for oxygen and iron are still larger than the predictions of Model A. So for the Milky Way disk, if the classical KS law of star formation is adopted, models are not able to reproduce enough of a disk abundance gradient, even if the infall time scale is radially dependent.

3) Although Model B can produce a reasonable value of the current gradient by properly adjusting the infall time scale, it predicts a much steeper gradient in the past. This is not supported by current available observations from planetary nebulae and open clusters. The steep abundance gradient at early times is due to the fact that the disk formation time scale in Model B is radial dependent which results in a delayed gas infall process and star formation in the outer disk.

4) Model C can predict not only the current values of abundance gradient along the Milky Way disk, but also the evolution of gradient which is fairly consistent with observations from PNe and OCs. Since the classical KS law was derived from the average SFR and gas mass surface densities for a whole galaxy (Kennicutt 1998), we expect that the modified KS star formation law, that is the radial dependent SFR, would be more suitable when we deal with the local star formation processes within a galaxy.

3.4. Comparison with Other Observations

Now we further compare the model results with other constraints, such as the gas, SFR and stellar profiles in the Milky Way disk. According to the discussions given above, the form and the value of infall time scale τ does not affect the radial profiles greatly, so we shall adopt $\tau(r) = 0.75 \times r + 1$. The results for all three models are presented in Fig. 3.

The observational data of current gas surface density Σ_{gas} come from Dame et al. (1993),

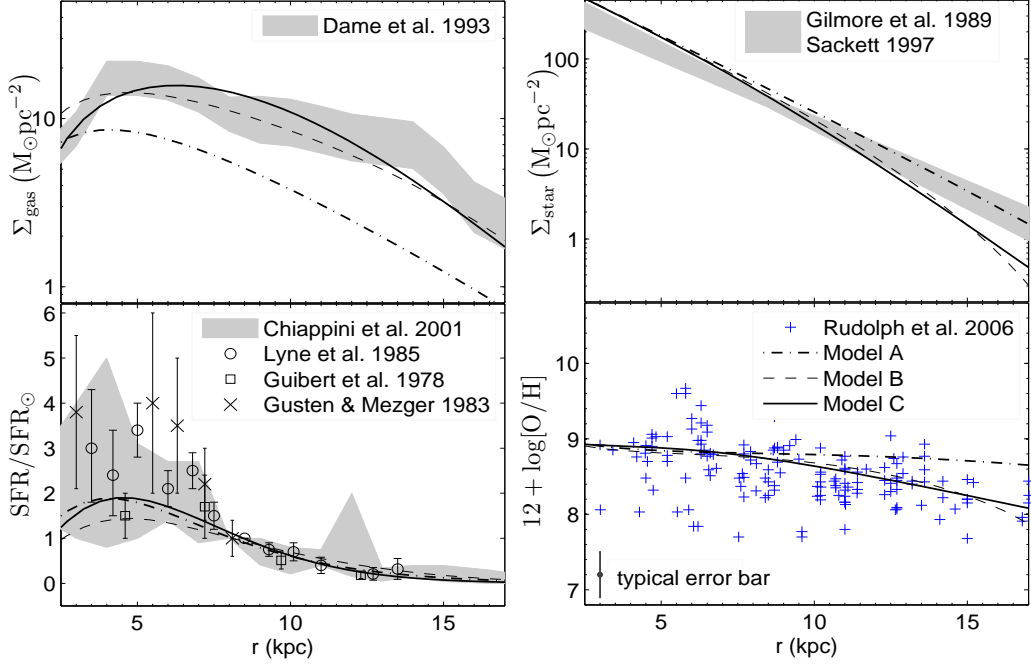


Fig. 3.— Comparison of Model A, B and C with the observed profiles of gas mass surface density, stellar mass surface density, star formation rate and oxygen abundance of the Milky Way disk (from top left to bottom right panel). The stellar mass surface density is obtained by assuming an exponential disk profile, where the stellar disk scale length $(r_d)_* = 2.5\text{--}3$ kpc (Sackett 1997) and the stellar mass surface density at the solar neighborhood $(\Sigma_{\text{star}})_\odot = 35 \pm 5 M_\odot \text{pc}^{-2}$ (Gilmore et al. 1989). For all three models, we adopt the infall time scale to be $\tau(r) = (0.75 \times r + 1)\text{Gyr}$.

$\text{SFR}/\text{SFR}_\odot$ from Gusten & Mezger (1983), Lyne et al. (1985), Guibert et al. (1978), and Chiappini et al. (2001). The data of Σ_{star} are from the solar neighbourhood value $(\Sigma_{\text{star}})_\odot = 35 \pm 5 M_\odot \text{pc}^{-2}$ (Gilmore et al. 1989) and extend to the whole disk with an exponential radial profile of stars, in which $(r_d)_* = 2.5 \sim 3$ kpc (Sackett 1997, Hammer et al. 2007). The oxygen abundance profile is from Rudolph et al. (2006).

From Fig. 3, we can see that, in general, all of the three models are able to predict a reasonable profile for Σ_{star} and $\text{SFR}/\text{SFR}_\odot$. Since the observed SFR and stellar mass surface density are quite uncertain, they are not good tracers to constrain model results. However, based on the observed gas and abundance profiles, it is clear that Mod-A is not a good choice since it is difficult to get acceptable matches to the data no matter how we modulate

infall time scale. But both model B and C are acceptable, and Model C is relatively much better, for it is consistent with the above discussions based on the past history of abundance gradient.

4. Summary

Based on a simple model of galactic chemical evolution, which includes infall, star formation and delayed disk formation, we have investigated the origin and evolution of the radial abundance gradient of a disk galaxy. By comparing the model results with the observations in the Milky Way disk, we try to find the effect of each mechanism on shaping abundance gradients and decide which one plays the main role.

The main results of our model can be summarized as follows:

1. For all adopted models and parameters, the predicted radial abundance gradients are steeper in the early epoch of disk evolution, which is consistent with observations of planetary nebulae and open clusters.
2. The disk formation time scale $t_0(r)$ could be the most important parameter governing the production of the abundance gradient, no matter what SFR and infall time scale are assumed. In this case, the inner disk accretes infalling gas earlier than the outer part, thus star formation and metal enrichment start earlier in the inner region. However, this will predict a very steep abundance gradient in the past, which is not consistent with the observations.
3. Besides $t_0(r)$, the radial dependence of SFR will further strengthen the gradient. If $t_0(r)$ is not considered (i.e. $\gamma = 0$ in Eq.(4)), SFR plays the main role in shaping the disk abundance gradient. We find that the radially dependent SFR $\Psi \propto \Sigma_{\text{gas}}^{1.4} r^{-1}$ is a suitable model to fit the observational data in the Milky Way disk, while the classical KS law $\Psi \propto \Sigma_{\text{gas}}^{1.4}$ without t_0 cannot produce a current abundance gradient steep enough to match those that have been observed in the Galactic disk from Cepheids and HII regions.
4. Relative to t_0 and SFR, the infall time scale τ only plays a minor role in shaping the abundance gradient. Given a certain SFR, the adopted form of $\tau(r)$ will not significantly change the gradient. But compared with constant infall time scale, an “inside-out” assumption for the time scale could help to produce some degree of abundance gradient.

5. When we divide the disk into inner and outer parts at the intersection radius of 8 kpc, our model predicts a steeper gradient in the outer disk. We note that there are observations showing a flatter abundance gradient for the outer Galactic disk based on different tracers, such as open clusters, Cepheids, and young stars. But there are also other independent studies that do not show evidence of a flattening gradient toward outer disk. Observations from Cepheids also show that the Galactic iron gradient might be more accurately described by a bimodal distribution, especially in the outer disk. All of those shows a complicated formation history of the outer Galactic disk. Further observational work and more sophisticated models need to be done before we can have a more clear understanding of the outer disk formation.

In summary, we expect that for an individual Milky Way type galaxy, a better description of the SFR is the modified KS star formation law. In fact, the modified KS law can also be written as $\Psi = \alpha(r)\Sigma_{\text{gas}}^{1.4}$. This is equivalent to classical KS law, only the normalization coefficient $\alpha(r)$ (which is related to star formation efficiency) is inversely proportional to the distance from the galaxy center. This kind of SFR could well reproduce the observed Galactic disk abundance gradient and its time evolution.

We are grateful to the critical comments from an anonymous referee. Eric Peng is thanked for his helpful comments on the writing of the paper. This work is supported by the National Science Foundation of China No.10573028, 10573022, the Key Project No.10833005, the Group Innovation Project No.10821302, and by 973 program No. 2007CB815402.

REFERENCES

- Andrievsky, S. M., Kovtyukh, V. V. & Luck, R. E., et al. 2002, *A&A*, 381, 32
- Andrievsky, S. M., Luck, R. E., Martin, P., & Lépine, J. R. D. 2004, *A&A*, 413, 159
- Azzollini, R., Trujillo, I. & Beckman, J. E. 2008, *ApJ*, 684, 1026
- Blair, W. P., Kirshner, R. P. & Chevalier, R. A. 1982, *ApJ*, 254, 50
- Blitz, L., Spergel, D. N. & Teuben, P. J. et al. 1999, *ApJ*, 514, 818
- Boissier, S. & Prantzos, N. 1999, *MNRAS*, 307, 857
- Boissier, S. & Prantzos, N. 2000, *MNRAS*, 312, 398
- Boissier, S. & Prantzos, N. 2001, *MNRAS*, 325, 321

- Boissier, S., Boselli, A., Prantzos, N. & Gavazzi, G. 2001, MNRAS, 321, 733
- Boissier, S., Gil de Paz, A., Boselli, A., Madore, B. & Buat, V. et al. 2007, ApJS, 173, 524
- Carraro, G., Geisler, D., Villanova, S., Frinchaboy, P. M. & Majewski, S. R. 2007, A&A, 476, 217
- Carraro, G., Ng, Y.K., Portinari, L. 1998, MNRAS, 296, 1045
- Chang, R. X., Hou, J. L., Shu, C. G. & Fu, C. Q. 1999, A&A, 350, 38
- Chen, L., Hou, J. L. & Wang, J. J. 2003, AJ, 125, 1397
- Chiappini, C., Matteucci, F. & Romano, D. 2001, ApJ, 554, 1044
- Costa, R. D. D., Uchida, M. M. M. & Maciel, W. J. 2004, A&A, 423, 199
- Daflon, S. & Cunha, K. 2004, ApJ, 617, 1115
- Dame, T.M. 1993, in Holt, S.S., Verter, F., eds., AIP Conf. Proc. 278, Back to the Galaxy, American Institute of Physics, New York, p.267
- de Grijs, R., Kregel, M. & Wesson, K. H. 2001, MNRAS, 324, 1074
- Dennefeld, M. & Kunth, D. 1981, AJ, 86, 989
- Deharveng L., Pena, M., Caplan, J. & Costero, R. 2000, MNRAS, 311, 329
- Ferguson A. M. N., Irwin M. J., Ibata R. A., Lewis G. F., Tanvir N. R. 2002, AJ, 124, 1452
- Franx, M., van Dokkum, P. G., Schreiber, N. M. F., Wuyts, S., Labbé, I., Toft, S. 2008, ApJ, 688, 770
- Friel, E.D. 1995, ARA&A, 33, 381
- Friel, E.D. 1999, Ap&SS, 265, 271
- Friel, E.D., Janes, K.A., Tavares, M., Scott, J., Katsanis, R., Lotz, J., Hong, L. & Miller N. 2002, AJ, 124, 2693
- Gilmore, G., Wyse, R, Kuijken, K., 1989 in Beckman, J., Pagel, B., eds. Evolutionary Phenomena in Galaxies, Cambridge Univ. Press, Cambridge, p. 172
- Guibert, J., Lequeux, J. & Viallefond, F. 1978, A&A, 68, 1
- Gusten, R. & Mezger, P. G. 1983, Vistas Astr., 26, 159

- Hammer, F., Puech, M., Chemin, L., Flores, H. & Lehnert, M. D. 2007, *ApJ*, 662, 322
- Holmberg, J. & Flynn, C. 2004, *MNRAS*, 352, 440
- Hou, J. L., Prantzos, N. & Boissier, S. 2000, *A&A*, 362, 921
- Hou, J. L. & Chang, R. X. 2001, *Progress in Astronomy*, 19(1), 68
- Hou, J. L., Chang, R. X. & Chen, L. 2002, *ChJAA*, 2, 17
- Hou, J. L., Shu, C. G., Shen, S. Y., Chang, R. X., Chen, W. P. & Fu, C. Q. 2005, *ApJ*, 624, 561
- Ibata, R. A., Chapman, S. & Ferguson, A. M. N. et al. 2005, *ApJ*, 634, 287
- Janes, K. A., Tilley C. & Lynga, G. 1988, *AJ*, 95, 771J
- Kennicutt, R. C. 1998, *ARA&A*, 36, 189
- Kennicutt, R. C., Calzetti D., Walter, F., Helou, G. & Hollenbach, D. J. et al. 2007, *ApJ*, 671, 333
- Kroupa, P., Tout C. & Gilmore G. 1993, *MNRAS*, 262, 545
- Lemasle, B., François, P., Bono, G., Mottini, M., Primas, F. & Romaniello, M. 2007, *A&A*, 467, 283
- Lemasle, B., François, P., Piersimoni, A., Pedicelli, S. & Bono, G. et al. 2008, *A&A*, 490, 613
- Lodders, K. 2003, *ApJ*, 591, 1220
- Lyne, A. G., Manchester, R. N. & Taylor, J. H. 1985, *MNRAS*, 213, 613
- Maciel, W. J., Costa, R. D. D., Uchida, M. M. M. 2003, *A&A*, 397, 667
- Maciel, W. J., Lago, L. G. & Costa, R. D. D. 2005, *A&A*, 433, 127
- Maciel, W. J., Lago, L. G. & Costa, R. D. D. 2006, *A&A*, 453, 587
- Magrini, L., Corbelli, E., Galli, D. 2007a, *A&A*, 470, 843
- Magrini, L., Vilchez, J. M., Mampaso, A., Corradi, R. L. M. & Leisy, P. 2007b, *A&A*, 470, 865
- Magrini, L., Sestito, P., Randich, S. & Galli, D. 2008, [arXiv/08120854](https://arxiv.org/abs/08120854)

- Matteucci, F. 2001, *The Chemical Evolution of the Galaxy* (Kluwer)
- Molla, M., Ferrini, F. & Diaz, A. I. 1997, *ApJ*, 475, 519
- Pagel B. E. J. *Revista Mexicana de Astronomía y Astrofísica* (ISSN 0185-1101), vol. 18, Sept. 1989, p. 161-172
- Pohlen, M., Dettmar, R. J. & Lütticke, R. et al. 2002, *A&A*, 392, 807
- Prantzos, N. 2008, in *Stellar Nucleosynthesis: 50 years after B2FH*, ed. C. Charbonnel & J. P. Zahn, *EAS Publication Series* 32, 311
- Robin, A. C., Haywood, M. & Creze, M. et al. 1996, *A&A*, 305, 125
- Rolleston, W. R. J., Smartt, S. J., Dufton, P. L. & Ryans, R. S. I. 2000, *A&A*, 363, 537
- Rosolowsky, E. & Simon, J. D. 2008, *ApJ*, 675, 1213
- Rošar, R., Victor, P. D. et al. 2008, *AJ*, 675, L65
- Rudolph, A. L., Fich, M. & Bell, G. R. et al. 2006, *ApJS*, 162, 346
- Sackett, P. D. 1997, *ApJ*, 483, 103
- Sancisi, R., Fraternali, F., Oosterloo, T. & van der Hulst, T. 2008, *A&ARv*, 15, 189
- Schmidt, M. 1959, *ApJ*, 129, 243S
- Thilker, D. A., Braun, R. & Walterbos, R. A. M. et al. 2004, *ApJL*, 601, 39
- Twarog, B. A., Ashman, K. M. & Antony-Twarog, B. J. 1997, *AJ*, 114, 2556
- van den Bergh, S. 2006, *AJ*, 132, 1571
- Vilchez, J. M. & Esteban, C. 1996, *MNRAS*, 280, 720
- Wolfe, A. M., Gawiser, E. & Prochaska, J. X. 2005, *ARA&A*, 43, 861
- Yin, J., Hou, J. L., Prantzos, N., Boissier, S. & Chang, R. X. 2009, to be submitted.
- Yong, D., Carney, B. W. & Teixeira de Almeida M. L. 2005, *AJ*, 130, 597
- Yong, D., Carney, B. W., Teixeira de Almeida M. L. & Pohl, B. L. 2006, *AJ*, 131, 2256